Available online at www.sciencedirect.com

ScienceDirect

Transportation Research Procedia 2 (2014) 477 – 485

Transportation Research Procedia

www.elsevier.com/locate/procedia

The Conference on Pedestrian and Evacuation Dynamics 2014 (PED2014)

Comparative study of macroscopic pedestrian models

Monika Twarogowska [a], Paola Goatin [b,*], Regis Duvigneau [b]

[a] *Istituto per le Applicazioni del Calcolo "M. Picone" CNR, Via della Ricerca Scientifica 1, 00133 Roma, Italy*
[b] *Inria Sophia Antipolis - Méditerranée, 2004, route des Lucioles – BP 93, 06902 Sophia Antipolis Cedex, France*

Abstract

We analyze numerically some macroscopic models of pedestrian motion to compare their capabilities of reproducing characteristic features of crowd behavior, such as travel times minimization and crowded zones avoidance, as well as complex dynamics like stop-and-go waves and clogging at bottlenecks. We compare Hughes' model with different running costs, a variant with local dependency on the density gradient proposed in Xia et al. (2009), and a second order model derived from the Payne-Whitham traffic model which has first been analyzed in Jiang et al. (2010). In particular, our study shows that first order models are incapable of reproducing stop-and-go waves and blocking at exits.

Peer-review under responsibility of Department of Transport & Planning Faculty of Civil Engineering and Geosciences Delft University of Technology

Keywords: macroscopic models; crowd dynamics; evacuation; conservation laws; eikonal equation; finite volume numerical schemes

1. Introduction

Macroscopic models of pedestrian flows see the crowd as a continuum medium characterized by averaged quantities such as density and mean velocity. Like their corresponding vehicular traffic models, they consist of partial differential equations derived from fluid dynamics and accounting for mass conservation and eventually a momentum balance equation. Macroscopic road traffic models have been introduced in the fifties by Lighthill and Whitham (1955) and Richards (1956) and are nowadays well established both from the mathematical point of view and the engineering applications. These models have been applied to pedestrian flows only recently, starting from Hughes (2002), who defined the crowd as a "thinking fluid" and introduced a model coupling a scalar conservation law relying on mass conservation with an eikonal equation describing the direction of motion based on the density distribution in the domain. The literature has known a fast development since, and currently includes gas dynamics equations (Bellomo and Dogbé (2008); Jiang et al. (2010)), gradient flow methods (Maury et al. (2010)), non linear conservation laws with non classical shocks (Colombo and Rosini (2005)), non-local flows (Colombo et al. (2012)) and time evolving measures (Piccoli and Tosin (2009)). All these models have been studied from the analytical and numerical points

* Corresponding author. Tel.: +33-4-92387834 ; fax: +33-4-92387980.
E-mail address: paola.goatin@inria.fr

Peer-review under responsibility of Department of Transport & Planning Faculty of Civil Engineering and Geosciences Delft University of Technology
doi:10.1016/j.trpro.2014.09.063

of view, with an accent on the characteristic features of the solutions and their capability of reproducing observed phenomena. Yet, to our knowledge, a rigorous validation against real data has not been performed.

The scope of this paper is to compare numerically some macroscopic models found in the literature. In particular, we are interested in studying three variants of Hughes' model, based on three distinct choices of the velocity vector field that result in different accounts of pedestrians distribution in the domain, see El-Khatib et al. (2013) for a similar study. This could model crowds behaving more or less nervously, as panic states are often characterized by phenomena like *"freezing by heating"* and *"ignorance of available exits"*, see Helbing et al. (2002). We will also consider a second order model derived from the Payne (1971) and Whitham (1974) model for vehicular traffic and recently adapted to pedestrian movements by Jiang et al. (2010). It consists of a 2×2 system coupling the mass conservation law with a momentum balance equation accounting for relaxation towards the desired velocity and an "internal pressure" term modeling repealing forces between individuals. As observed by the authors in Twarogowska et al. (2014), this model presents interesting features compared to first order models, such as the presence of stop-and-go waves and blocking phenomena at bottlenecks, that can be solved by the presence of obstacles before the exits. In particular, this model is a good candidate to describe the so-called Braess' paradox, in which the presence of obstacles indeed improves the outflow and reduces the evacuation time, see again Helbing et al. (2002).

The simulations presented in this paper are run on two dimensional, continuous walking domains with impenetrable walls and exits as pedestrians' destination. Previous results on Hughes' model concern simulations of flow of pedestrians on a large platform with an obstacle in its interior, see Huang et al. (2009); Jiang et al. (2011). In the case of the second order model, Jiang et al. Jiang et al. (2010) considered the same domain and showed numerically the formation of stop-and-go waves. On the contrary, we are interested in analyzing evacuation situations. Indeed, this problem is an important safety issue because high pedestrians concentrations can build up in front of the exit, which can slow down the outflow and eventually result in major accidents due to the pressure in the crowd. Some experimental studies have been conducted in this direction, see Kretz et al. (2006); Seyfried et al. (2009); Hoogendoorn and Daamen (2005), but they face difficulties in reproducing realistic panic behavior. Numerical simulations are mainly available in the microscopic framework, see Helbing et al. (2000); Helbing and Johansson (2009); Helbing et al. (2005).

Numerical simulations are based on first order finite volume methods on unstructured triangular meshes, coupled with a finite element method for solving the eikonal equation. The resulting numerical schemes have been extensively analyzed by the authors in Twarogowska et al. (2013). Similar and higher order methods for macroscopic models of pedestrian flows have been previously developed by Huang et al. (2009) and Xia et al. (2008, 2009).

The paper is organized as follows. Section 2 describes the four macroscopic models that are subject to investigation. In Section 3 we describe the numerical schemes used for running simulations. Numerical tests are illustrated in Section 4 and conclusions are deferred to Section 5.

2. Macroscopic models

We consider a two dimensional connected domain $\Omega \subset \mathbb{R}^2$ corresponding to some walking facility equipped with one or more exits. The boundary of the domain $\partial\Omega = \Gamma_o \cup \Gamma_w$ consists of the outflow boundary denoted by Γ_o and the walls Γ_w. Macroscopic models derived from fluid dynamics consist of the mass conservation equation

$$\partial_t \rho + \mathrm{div}_{\mathbf{x}}\,(\rho \vec{v}) = 0, \qquad t > 0, \mathbf{x} \in \Omega, \tag{1}$$

where $\rho = \rho(t, \mathbf{x})$ is the pedestrian density and $\vec{v} = \vec{v}(t, x) \in \mathbb{R}^2$ is the mean velocity. The equation is closed either by a phenomenological relation that defines the vector field $\vec{v} = V(\rho)\vec{\mu}$ in the so-called *first-order models*, or by an additional momentum balance equation that accounts for acceleration in *second-order models*.

The speed function $V(\rho) : [0, \rho_{\max}] \to \mathbb{R}^+$ is assumed to be decreasing, see Buchmueller and Weidmann (2006). For our simulations we choose the exponential dependence

$$V(\rho) = v_{\max} e^{-\alpha\left(\frac{\rho}{\rho_{\max}}\right)^2}, \tag{2}$$

where $v_{\max}$ is the free flow speed, $\rho_{\max}$ is the congestion density and α is a positive constant.

Following Hughes (2002), the desired direction vector field $\vec{\mu}$ is often defined though the gradient of a scalar potential ϕ

$$\vec{\mu} = -\frac{\nabla\phi}{\|\nabla\phi\|}. \tag{3}$$

The function ϕ is the solution of an eikonal equation which accounts for the instantaneous minimum travel cost. It is given by

$$\begin{cases} \|\nabla\phi\| = c(t,\mathbf{x}) & \text{for } t > 0, \mathbf{x} \in \Omega, \\ \phi = 0 & \text{for } \mathbf{x} \in \Gamma_o. \end{cases} \tag{4}$$

Above, the running cost $c = c(t,\mathbf{x}) \in [1, +\infty[$ represents the cost of passing at point $\mathbf{x}$ at time t. In particular, taking

$$c(t,\mathbf{x}) \equiv 1, \tag{5}$$

the solution of (4) is $\phi(\mathbf{x}) = \text{dist}(\mathbf{x}, \Gamma_o)$, the distance of point $\mathbf{x}$ to the target Γ_o in the case of convex domains. Conversely, taking $c = c(\rho(t,x))$ as an increasing function of the density, the resulting vector field $-\nabla\phi/\|\nabla\phi\|$ "avoids" high density regions. This is the case of Hughes' model, where

$$c(t,x) = 1/V(\rho(t,x)). \tag{6}$$

The above choice implies that pedestrians have a knowledge of the density distribution in the whole domain at each time instant, and use this to estimate their travel time. This assumption is unrealistic in extended domains, where the restricted visibility of individuals makes the overview of the whole area impossible. For this reason, Xia et al. (2009) introduced a model with memory effect, in which pedestrians aim at following the shortest path to the destination based on the memory of its location, and temper their behavior locally to avoid high densities. This leads to define

$$\vec{\mu} = \frac{-\nabla\phi - \omega\nabla[V(\rho)^{-1} + g(\rho)]}{\left\|-\nabla\phi - \omega\nabla[V(\rho)^{-1} + g(\rho)]\right\|}, \tag{7}$$

where ϕ solves (4)-(5), $\omega > 0$ is a parameter expressing the psychological repulsion and $g(\rho) = \beta\rho^2$ is a discomfort field function depending on a parameter $\beta > 0$ that accounts for the sensitivity of pedestrians to comfort level.

Second order models, which are quite common for vehicular traffic, see for example Aw and Rascle (2000) and Blandin et al. (2011), have been adapted to crowd models in Jiang et al. (2010). They consider the Payne (1971) and Whitham (1974) model, which couples the mass conservation equation (1) with the following momentum balance

$$\partial_t(\rho\vec{v}) + \text{div}_{\mathbf{x}}(\rho\vec{v}\otimes\vec{v}) = \frac{1}{\tau}\rho\left(V(\rho)\vec{\mu} - \vec{v}\right) - \nabla P(\rho). \tag{8}$$

Above, the parameter τ is a relaxation time at which pedestrians adapt their current velocity $\vec{v}$ to the desired one $V(\rho)\vec{\mu}$, whose direction $\vec{\mu}$ is given by (3)-(4)-(5). The second term in the right hand side of (8) is a repulsive force modeling the volume filling effect and is given by the power law for isentropic gases

$$P(\rho) = p_0\rho^\gamma, \qquad p_0 > 0, \gamma > 1. \tag{9}$$

3. Numerical schemes

To discretize the models described in the previous section, we use finite volume schemes for equations (1) and (8), and a finite element method based on the variational principle to solve the eikonal equation (4). Both schemes are developed on unstructured triangular meshes.

3.1. Finite volume schemes for the macroscopic models

We decompose the domain Ω into N non overlapping, finite volume cells C_i, $i = 1, ..., N$, given by dual cells centered at vertices of the triangular mesh. For each cell C_i we consider a set of N_i neighbouring cells C_{ij}, $j = 1, ..., N_i$.

By e_{ij} we denote the face between C_i and C_{ij}, $|e_{ij}|$ its length and $\vec{n}_{ij}$ is a unit vector pointing from the center of the cell C_i towards the center of the cell C_{ij}. The solution U on a cell C_i is approximated by the cell average of the solution at time $t > 0$, that is

$$U_i = \frac{1}{|C_i|} \int_{C_i} U(x,t)\, dx.$$

The numerical approximation at cell C_i of the solution to the mass conservation equation (1) ρ_i is obtained using Lax-Friedrichs scheme

$$\rho_i^{n+1} = \rho_i^n - \frac{\Delta t}{|C_i|} \sum_{j=1}^{N_i} |e_{ij}| \mathcal{F}(\rho_i^n, \rho_j^n, \vec{n}_{ij}), \qquad \text{whith} \quad \mathcal{F}\left(\rho_i, \rho_j, \vec{n}_{ij}\right) = \frac{1}{2}\left[G(\rho_i)\cdot\vec{n}_{ij} + G(\rho_j)\cdot\vec{n}_{ij} - \xi(\rho_j - \rho_i)\right], \tag{10}$$

where $G(\rho) = \rho V(\rho)\vec{\mu}$ and the numerical viscosity coefficient ξ is given by

$$\xi = \max_{l=i,j} \left| \frac{d}{d\rho} G(\rho_l) \right| = \max_{l=i,j} \left| \frac{d}{d\rho} \left(\rho_l V(\rho_l)\vec{\mu}_l(\rho)\right) \right| = \max_{l=i,j} \left| \frac{d}{d\rho} \left(\rho_l V(\rho_l)\right) \right|.$$

Stability is achieved under the CFL condition $\Delta t < \min_{i=1,\dots,N} \text{diameter}(C_i)/v_{\max}$.

The second order model (1)-(8) can be put in the form

$$\partial_t U + \text{div}_{\mathbf{x}} \vec{F}(U) = S(U), \tag{11}$$

where $U = (\rho, \rho\vec{v})^T$ denotes the unknowns vector and

$$\vec{F}(U) = \begin{pmatrix} F^{\rho} \\ F^{\rho\vec{v}} \end{pmatrix} = \begin{pmatrix} \rho\vec{v} \\ \rho\vec{v}\otimes\vec{v} + P(\rho) \end{pmatrix}, \qquad S(U) = \begin{pmatrix} 0 \\ \frac{1}{\tau}\rho\left(V(\rho)\vec{\mu} - \vec{v}\right) \end{pmatrix}.$$

The homogeneous part of the model (11) coincides with the isentropic gas dynamics system for which many solvers are available, see Toro (2009). However, the occurrence of vacuum may cause instabilities and not all the schemes preserve non-negativity of the density. We use the first order HLL approximate Riemann solver of Harten et al. (1983). It assumes that the solution consists of three constant states separated by two waves with speeds σ_L and σ_R corresponding respectively to the slowest and fastest signal speeds. It preserves non-negativity of the density under certain conditions on the above numerical wave speeds, see Einfeldt et al. (1991).

Due to the coupling with the eikonal equation (4), we apply explicit time integration to (11), resulting in a splitting between the transport and the source terms

$$\begin{cases} U_i^* = U_i^n - \dfrac{\Delta t}{|C_i|} \displaystyle\sum_{j=1}^{N_i} |e_{ij}| \mathcal{F}(U_i^n, U_j^n, \vec{n}_{ij}), \\ U_i^{n+1} = U_i^* + \Delta t S(U_i^*). \end{cases} \tag{12}$$

The stability of the scheme is assured by the CFL condition $\Delta t < \min_{i=1,\dots,N} \text{diameter}(C_i)/\sigma_i$, where σ_i is the maximal value of the characteristic wave speed of the homogeneous part of the system (11) and is given by

$$\sigma_i = \max_{j=1,\dots,N_i} (\vec{v}_i \cdot \vec{n}_{ij}) + \sqrt{P'(\rho_i)}.$$

3.2. Eikonal equation

To obtain the solution at time step t^{n+1} we need to compute the direction vector $\vec{\mu}$ defined by (3). It means that we have to solve the eikonal equation (4) and compute the gradient of its solution. We implement the Bornemann and Rasch (2006) algorithm, which is a finite element scheme and thus easier to implement on unstructured triangular meshes with respect to other methods available in the literature. It is a linear, finite element discretization based on the solution to a simplified, localized Dirichlet problem solved by the variational principle (for details see Twarogowska et al. (2013)).

Once computed the potential approximations ϕ_i at each node of the mesh, we calculate its gradient using the nodal P_1 Galerkin gradient method. It is related to cell C_i and is computed by averaging the gradients of all triangles having node i as a vertex. In two dimensions it has the form

$$\nabla\phi_i = \frac{1}{|C_i|}\sum_{T_{ij}\in C_i}\frac{|T_{ij}|}{3}\sum_{k\in T_{ij}}\phi_k\nabla P_k|_{T_{ij}}, \tag{13}$$

where T_{ij} are finite elements with the considered node i as a vertex, k counts for vertices of T_{ij} and $P_k|_{T_{ij}}$ is a P_1 basis function associated with vertex k.

3.3. Boundary conditions

We set the outflow boundary Γ_o far from the exit of the room through which pedestrians move, so that the outflow rate doesn't influence the flow through the door. On the walls, we impose free-slip boundary conditions

$$\vec{v}\cdot\vec{n} = 0, \quad \frac{\partial\rho}{\partial n} = 0 \qquad \text{at } \Gamma_w. \tag{14}$$

For the first order models (1), boundary conditions are imposed by defining directly the fluxes at boundary facets. More precisely, we set

$$\mathcal{F} = \begin{cases} 0 & \text{at } \Gamma_w \\ \rho_{\max}V(\rho_{\max}) & \text{at } \Gamma_o \end{cases}. \tag{15}$$

For the second order model (1)-(8), we extend the domain defining ghost states given by

$$\rho_g = \rho_i, \qquad \vec{v}_g = \vec{v}_i - 2(\vec{v}_i\cdot\vec{n})\,\vec{n} \tag{16}$$

at wall boundary Γ_w and

$$\rho_g = 0.1\,\rho_{\max}, \qquad \vec{v}_g = v_{\max}\vec{n} \tag{17}$$

for the outflow Γ_o.

3.4. Initial conditions

In our simulations we consider initial conditions of the form

$$\rho_0(x) = \begin{cases} \bar{\rho} \text{ in } \Omega_0 \\ 0 \text{ elsewhere} \end{cases}, \qquad \vec{v}_0(x) = 0, \tag{18}$$

where $\bar{\rho}$ is a positive constant and Ω_0 is an area inside the evacuation domain Ω.

4. Numerical tests

In this section we present the result of some numerical simulations of evacuation dynamics of pedestrians from a corridor and a room. In particular, we are interested in comparing the various models described in Section 2. We will see that first order models cannot reproduce complex dynamics such as the formation of stop-and-go waves and clogging at bottlenecks. On the other hand, the second order model (1)-(8) shows interesting behavior in the presence of obstacles in front of exits, that could regularize the flow, decrease the inter-pedestrian pressure and facilitate evacuation.

In the following numerical simulations we have used the choices for the parameters listed in Table 1. Maximal velocity $v_{\max}$, maximal density ρ_{max} and the response time τ are chosen from the available literature on experimental studies of pedestrian behavior (see Buchmueller and Weidmann (2006); Seyfried et al. (2006)). The values of some of the parameters of the second order model (1)-(8), such as p_0, γ, α to authors' knowledge do not have a direct correspondence with the microscopic characteristics of pedestrian motion.

We use the following functionals and corresponding discrete versions to evaluate the models performances:

Table 1. Parameters values used in the numerical simulations

Parameter name	Symbol	Value	Units
desired speed	$v_{\max}$	2	m/s
relaxation time	τ	0.61	s
maximal density	$\rho_{\max}$	6 – 10	ped/m^2
pressure coefficient	p_0	0.005	$\mathrm{ped}^{1-\gamma} \cdot m^{2+\gamma}/s^2$
adiabatic exponent	γ	2	-
density-speed coefficient	α	7.5	-

- Total mass of pedestrians inside the evacuation domain

$$M(t) = \int_\Omega \rho(x,t)dx, \qquad M^n = \sum_{i=1}^{N} \rho_i^n |C_i|. \tag{19}$$

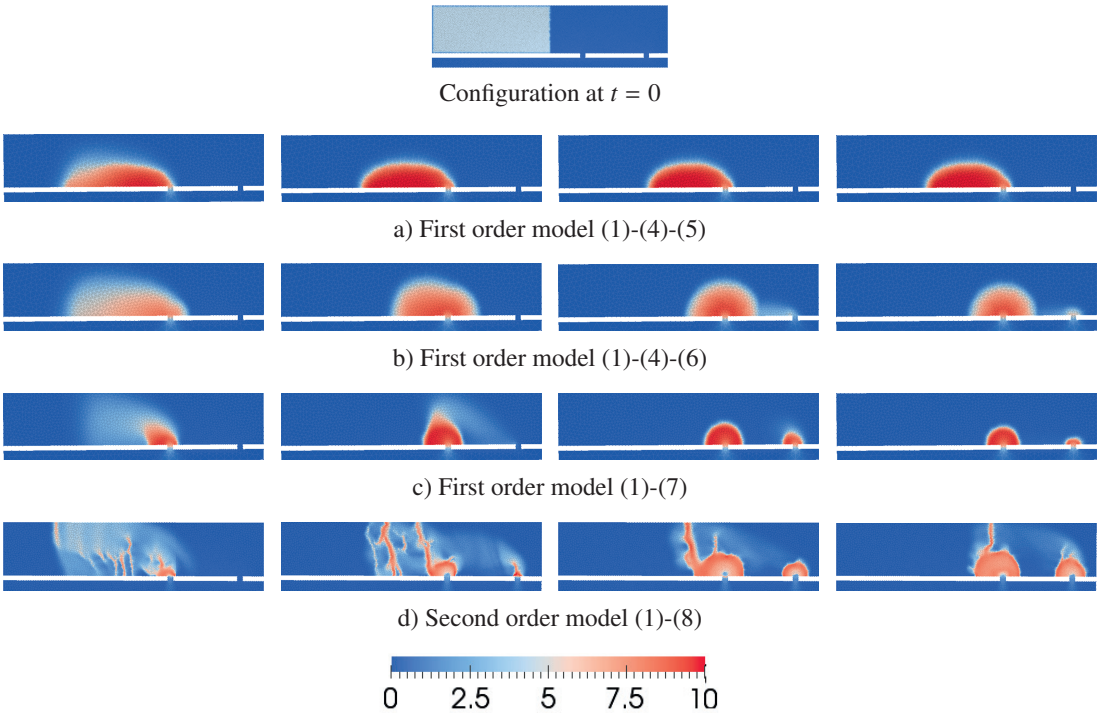

Fig. 1. Initial density at $t = 0s$ (top) and density evolutions corresponding to the models described in Section 2 at times $t = 20s,\ 40s,\ 60s,\ 80s$.

4.1. Test 1: corridor evacuation with two exits

We consider a corridor $100m \times 20m$ with two $1.2m$ wide exits centered symmetrically at $x = 67m$ and $x = 93m$. The initial density is $\rho_0 = 3\mathrm{ped}/m^2$ in the region $[0m, 50m] \times [6m, 26m]$ and zero elsewhere, see Fig. 1. The maximal density value is set $\rho_{\max} = 10$ in these tests.

Fig. 1 shows the densities corresponding to the four models described in Section 2 at times $t = 20s,\ 40s,\ 60s,\ 80s$. As expected, the first order model (1)-(4)-(5), representing people following the shortest path, neglects the second exit, thus resulting in a much longer evacuation time, see Fig. 1a. All the other models, instead, distribute the mass among the two exits, resulting in lower density values and better evacuation flows. In particular, the second order model (1)-(8) displays interesting features such as the formation of stop-and-go waves and arcs near the exits, due to strong interactions between individuals, measured by the the parameter p_0, see Twarogowska et al. (2014) for further details abut the role of the pressure parameter and the backward propagation of stop-and-go waves.

4.2. Test 2: room evacuation with obstacle

We consider a room represented by the domain $\Omega = [0m, 10m] \times [0m, 6m]$ with an exit of width $L = 1.6m$ centered at $(x, y) = (10m, 3m)$. The initial density $\rho(0, \mathbf{x})$ is set equal to $\rho_0 = 3\text{ped}/m^2$ in the region $[1m, 5m] \times [1m, 5m]$, and zero elsewhere. We are interested in measuring the effect of the presence of a circular column of radius $r = 0.5m$ centered at $(x, y) = (8.5m, 3.2m)$, see Fig. 2, top. The maximal density value is here taken $\rho_{\max} = 6$.

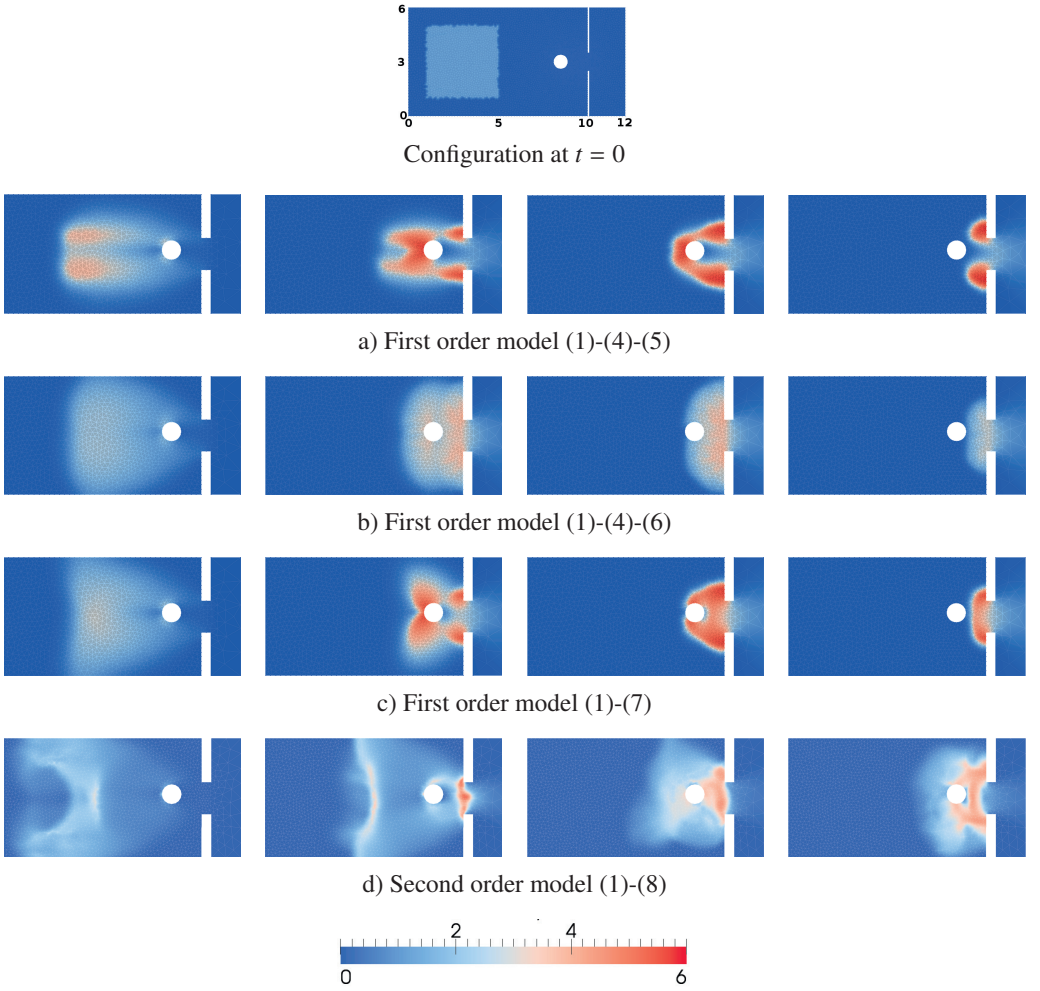

Fig. 2. Initial density at $t = 0s$ (top) and density evolutions corresponding to the models described in Section 2 at times $t = 2s,\ 5s,\ 8s,\ 11s$.

We run simulations for the models presented in Section 2. The density evolution is depicted in Fig. 2 at times $t = 2s,\ 5s,\ 8s$ and $11s$, showing the differences in the corresponding motion. In particular, the first order model shows greater density values behind the column and at the exit corners, corresponding to pedestrians that do not adapt their trajectory to the presence of other people and resulting in longer evacuation times, see Fig. 3. On the other hand, Hughes' model (Fig. 2b) displays greater diffusion and lower densities, even compared to the dynamic model with memory effect (7) in Fig. 2c, which has an intermediate behavior between (1)-(4)-(5) and (1)-(4)-(6).

The behavior displayed by the second order model (1)-(8) is quite different. First of all, we can observe the formation of stop-and-go waves even far from the exit, and arcs formation between the exit and the column, see Fig. 2d. Moreover, the total mass (19) time evolution depicted in Fig. 3, right, shows that the outflow is slowed down twice, but the presence of the column has a regularizing effect and slightly decreases the final evacuation time. In any case, the evacuation time is much longer than the one given by first order models (Fig. 3, left).

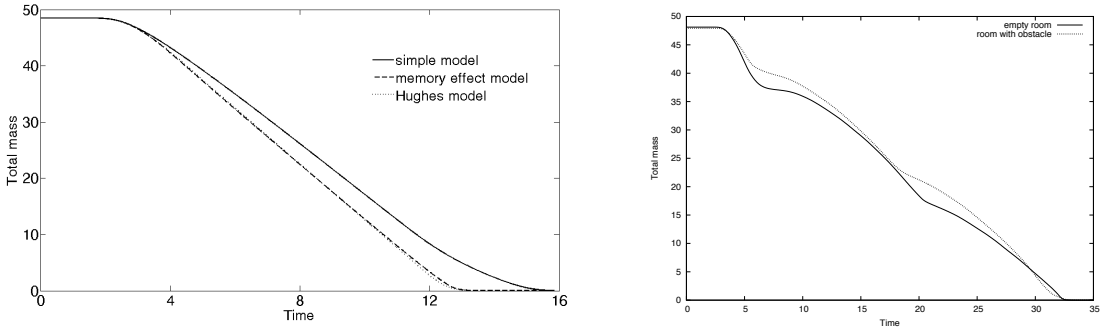

Fig. 3. Total mass (19) evolution corresponding to the simulations depicted in Fig. 2. Left: first order models with column. Right: second order model with and without column.

5. Conclusions

The tests presented in this paper show that the macroscopic approach to pedestrian flow modeling can capture a variety of aspects that characterize crowd behavior. In this sense, macroscopic models are easily adaptable to various situations and circumstances by simply changing the running cost in (4) accordingly. More complex behaviors like stop-and-go waves and clogging at bottlenecks can be simulated using the second order model (1)-(8).

Possible directions of future research include the use of different vector fields for the desired velocity direction $\vec{\mu}$ in the second order model, obtained for example using (5) or (7), and comparison with the non-local models introduced by Colombo et al. (2012) and Colombo and Lécureux-Mercier (2012). Finally, all these models need to be calibrated and validated on real data.

Acknowledgements

This research was supported by the European Research Council under the European Union's Seventh Framework Program (FP/2007-2013) / ERC Grant Agreement n. 257661.

References

Aw, A., Rascle, M., 2000. Resurrection of "second order" models of traffic flow. SIAM J. Appl. Math. 60, 916–938 (electronic).

Bellomo, N., Dogbé, C., 2008. On the modelling crowd dynamics from scaling to hyperbolic macroscopic models. Math. Models Methods Appl. Sci. 18, 1317–1345.

Blandin, S., Work, D., Goatin, P., Piccoli, B., Bayen, A., 2011. A general phase transition model for vehicular traffic. SIAM J. Appl. Math. 71, 107–127.

Bornemann, F., Rasch, C., 2006. Finite-element discretization of static Hamilton-Jacobi equations based on a local variational principle. Comput. Vis. Sci. 9, 57–69.

Buchmueller, S., Weidmann, U., 2006. Parameters of Pedestrians, Pedestrian Traffic and Walking Facilities. Schriftenreihe des IVT, Institute for Transport Planning and Systems (IVT), Chair of Transport Systems, ETH Zurich.

Colombo, R., Rosini, M., 2005. Pedestrian flows and nonclassical shocks 28, 1553–1567.

Colombo, R.M., Garavello, M., Lécureux-Mercier, M., 2012. A class of nonlocal models for pedestrian traffic. Math. Models Methods Appl. Sci. 22, 1150023, 34.

Colombo, R.M., Lécureux-Mercier, M., 2012. Nonlocal crowd dynamics models for several populations. Acta Math. Sci. Ser. B Engl. Ed. 32, 177–196.

Einfeldt, B., Munz, C.D., Roe, P.L., Sjögreen, B., 1991. On Godunov-type methods near low densities. J. Comput. Phys. 92, 273–295.

El-Khatib, N., Goatin, P., Rosini, M.D., 2013. On entropy weak solutions of Hughes' model for pedestrian motion. Z. Angew. Math. Phys. 64, 223–251.

Harten, A., Lax, P.D., Leer, B.v., 1983. On Upstream Differencing and Godunov-Type Schemes for Hyperbolic Conservation Laws. Siam Review 25. doi:10.1137/1025002.

Helbing, D., Buzna, L., Johansson, A., Werner, T., 2005. Self-organized pedestrian crowd dynamics: Experiments, simulations, and design solutions. Transportation Science 39, 1–24.

Helbing, D., Farkas, I., Molnàr, P., Vicsek, T., 2002. Simulation of pedestrian crowds in normal and evacuation situations, in: Schreckenberg, M., Sharma, S.D. (Eds.), Pedestrian and Evacuation Dynamics, Springer. pp. 21–58.

Helbing, D., Farkas, I., Vicsek, T., 2000. Simulating Dynamical Features of Escape Panic. Nature 407, 487–490.

Helbing, D., Johansson, A., 2009. Pedestrian, crowd and evacuation dynamics., in: Meyers, R.A. (Ed.), Encyclopedia of Complexity and Systems Science. Springer, pp. 6476–6495.

Hoogendoorn, S., Daamen, W., 2005. Pedestrian behavior at bottlenecks. Transportation Science 39, 147–159.

Huang, L., Wong, S., Zhang, M., Shu, C.W., Lam, W., 2009. Revisiting hughes' dynamic continuum model for pedestrian flow and the development of an efficient solution algorithm. Transportation Research Part B: Methodological 43, 127–141.

Hughes, R.L., 2002. A continuum theory for the flow of pedestrians. Transportation Research Part B: Methodological 36, 507 – 535.

Jiang, Y., Zhang, P., Wong, S., Liu, R., 2010. A higher-order macroscopic model for pedestrian flows. Physica A: Statistical Mechanics and its Applications 389, 4623 – 4635.

Jiang, Y.Q., Liu, R.X., Duan, Y.L., 2011. Numerical simulation of pedestrian flow past a circular obstruction. Acta Mech. Sin. 27, 215–221.

Kretz, T., Grünebohm, A., Schreckenberg, M., 2006. Experimental study of pedestrian flow through a bottleneck. Journal of Statistical Mechanics: Theory and Experiment 2006, P10014.

Lighthill, M.J., Whitham, G.B., 1955. On kinematic waves. II. A theory of traffic flow on long crowded roads. Proceedings of the Royal Society of London. Series A. Mathematical and Physical Sciences 229, 317.

Maury, B., Roudneff-Chupin, A., Santambrogio, F., 2010. A macroscopic crowd motion model of gradient flow type. Math. Models Methods Appl. Sci. 20, 1787–1821.

Payne, H., 1971. Models of Freeway Traffic and Control. Simulation Councils, Incorporated.

Piccoli, B., Tosin, A., 2009. Pedestrian flows in bounded domains with obstacles. Contin. Mech. Thermodyn 21, 85–107.

Richards, P., 1956. Shock waves on the highway. Operations research 4, 42–51.

Seyfried, A., Passon, O., Steffen, B., Boltes, M., Rupprecht, T., Klingsch, W., 2009. New insights into pedestrian flow through bottlenecks. Transportation Science 43, 395–406.

Seyfried, A., Steffen, B., Lippert, T., 2006. Basics of modelling the pedestrian flow. Physica A 368, 232–238.

Toro, E., 2009. Riemann Solvers and Numerical Methods for Fluid Dynamics: A Practical Introduction. Springer-Verlag Berlin Heidelberg.

Twarogowska, M., Goatin, P., Duvigeau, R., 2014. Macroscopic modelling and simulation of room evacuation. Appl. Math. Model. .

Twarogowska, M., Goatin, P., Duvigneau, R., 2013. Numerical study of macroscopic pedestrian flow models. Rapport de recherche RR-8340. INRIA. URL: http://hal.inria.fr/hal-00849587.

Whitham, G., 1974. Linear and nonlinear waves. Pure and applied mathematics, Wiley.

Xia, Y., Wong, S.C., Shu, C., 2009. Dynamic continuum pedestrian flow model with memory effect. Phys. Rev. E 79, 066113.

Xia, Y., Wong, S.C., Zhang, M., Shu, C.W., Lam, W.H.K., 2008. An efficient discontinuous Galerkin method on triangular meshes for a pedestrian flow model. Internat. J. Numer. Methods Engrg. 76, 337–350.